

# THE THERMAL AND MAGNETIC PROPERTIES OF SOME RARE EARTH-Pd<sub>3</sub> PHASES OF THE AuCu<sub>3</sub> STRUCTURE

J. M. MACHADO DA SILVA \*

Clarendon Laboratory, Parks Road, Oxford OX13PU U.K.

W. E. GARDNER

Materials Physics Division, AERE, Harwell, Oxon, U. K.

I. R. HARRIS

Department of Physical Metallurgy and Science of Materials, Birmingham University, Birmingham B15 2TT, UK.

(Received 30 June 1981)

*Abstract*—Heat capacity and magnetization measurements have been made on LaPd<sub>3</sub>, PrPd<sub>3</sub>, TbPd<sub>3</sub> and ErPd<sub>3</sub>. Values of  $\gamma = 0.33 \pm 0.02$  mJ/(K<sup>2</sup>. g atom) and  $\Theta_D = 171 \pm 1$  K were found for LaPd<sub>3</sub>. In the other phases specific heat contributions from both magnetic ordering and crystal field levels were observed:  $T_N = 0.6$  K and  $E(\Gamma_3) - E(\Gamma_5) = 4$  K for PrPd<sub>3</sub>;  $T_N = 3.7$  K and  $E(\Gamma_5) - E(\Gamma_3) = 8$  K for TbPd<sub>3</sub>;  $T_N < 0.22$  K and  $E(\Gamma_8^{(3)}) - E(\Gamma_6) = 2$  K for ErPd<sub>3</sub>.

Saturation moments at 1.2 K and in effective fields of 37 kOe of 0.97, 6.60 and 7.52  $\mu_B$  were observed for PrPd<sub>3</sub>, TbPd<sub>3</sub> and ErPd<sub>3</sub> respectively. The results have been analysed using a crystal field Hamiltonian and compared with the predictions of a simple point-charge model.

## 1 — INTRODUCTION

Rare earth metals form intermetallic compounds of the AuCu<sub>3</sub> type (L1<sub>2</sub>) with Al, Pd, In, Sn, Pt, Tl and Pb [1]. The magnetic properties of several of these compounds [2], [3], [4] have been reported and it is noticeable that, for a given rare earth atom, the ordering temperature is about an order of magnitude smaller

---

(\*) Now at Centro de Física da Universidade do Porto (INIC), Faculdade de Ciências, 4000 Porto, Portugal.

for the palladium-based phases. Thus these phases offer the opportunity to examine the properties of the rare earth atoms in environments where the crystal field interaction predominates over the exchange interaction. Both heat capacity and magnetic measurements can lead to estimates of the crystal field and exchange interactions.

## 2 — EXPERIMENTAL

The details of sample preparation have been given previously by Gardner *et al* [2]. The magnetic measurements have been made using a Sartorius electronic microbalance and a superconducting solenoid with gradient coils [5] in fields up to 42 kOe and at temperatures between 1 and 50 K. Heat capacity measurements have been made using the technique and equipment described previously [6].

## 3 — THEORY

### 3.1. Heat Capacity

For a metallic lattice with 4 atoms / unit cell the heat capacity / g molecule at low temperature is given by

$$C_v = 7776 (T/\theta_D)^3 + 4\gamma T \quad \text{J mole}^{-1} \text{K}^{-1} \quad (1)$$

where  $\theta_D$  is the Debye temperature and  $\gamma$  the coefficient of the electronic heat capacity of 1 g atom [7].

Although the 4f electron is not localized in CePd<sub>3</sub> [2] the magnetic evidence suggests that the 4f electrons are localized in the succeeding phases of the rare earth series. All the other rare earth ions, including europium, are trivalent in the RPd<sub>3</sub> phases and the 4f<sup>n</sup> free ion ground level is split in these AuCu<sub>3</sub> intermetallic phases by the cubic crystalline field from the neighbours. These splittings can be calculated by solving the crystal field Hamiltonian.

The crystal field Hamiltonian can be written in many equivalent forms using various related parameters. For a rare earth

ion in a cubic crystalline field we have chosen to express the Hamiltonian in angular momentum operators with respect to a polar axis of quantization  $z$ , which can have 2 - ( $\langle 110 \rangle$  direction), 3 - ( $\langle 111 \rangle$  direction) or 4 - ( $\langle 100 \rangle$  direction) fold symmetry :

$$\mathcal{H} = B_4 (O_4^0 + 5 O_4^4) + B_6 (O_6^0 - 21 O_6^4) \quad (2)$$

where

$$B_4 = A_4 \langle r^4 \rangle \beta, \quad B_6 = A_6 \langle r^6 \rangle \gamma \quad (3)$$

i.e.

$$\mathcal{H} = A_4 \langle r^4 \rangle \beta (O_4^0 + 5 O_4^4) + A_6 \langle r^6 \rangle \gamma (O_6^0 - 21 O_6^4) \quad (4)$$

where the  $O_n^m$  are Stevens operator equivalents, and  $\beta$  and  $\gamma$  are Stevens multiplicative factors [8], [9].

The quantities  $A_4 \langle r^4 \rangle$  and  $A_6 \langle r^6 \rangle$  are the crystal field parameters which determine the magnitude of the splittings and the matrix elements.

These parameters can be regarded as empirical ones or calculated from a point charge model. For the RPd<sub>3</sub> phases the simple point charge model can be evaluated in terms of the unit cell dimension  $a$  and charges  $Z_1$  on the 12 nearest-neighbors Pd atoms at a distance  $a/\sqrt{2}$  and  $Z_2$  on the 6 R-neighbors at distance  $a$ . The appropriate relations are [10] (hereafter denoted by LLW)

$$B_4 = (7/16) (e^2/a^5) (2\sqrt{2} Z_1 - Z_2) \langle r^4 \rangle \beta \quad (5)$$

$$B_6 = (3/64) (e^2/a^7) (26\sqrt{2} Z_1 - Z_2) \langle r^6 \rangle \gamma \quad (6)$$

LLW use the two alternative parameters  $W$ , which is the energy scale factor, and  $x$ , which measures the relative size of the fourth- and sixth-degree terms, where

$$B_4 F(4) = W x \quad (7)$$

$$B_6 F(6) = W (1 - |x|) \quad (8)$$

F(4) and F(6) are numerical factors introduced for convenient pictorial representation and tabulated by LLW.

LLW have essentially diagonalized eq. (4) for all values of  $x$  and all  $J$  and have reported the energies of the crystal field states and their wave functions. (The energies are, of course, independent of the choice of axis of quantization but the wave functions are not). Thus if the energies of these states are measured,  $x$  and  $W$  may be obtained from LLW and the fourth and sixth-degree terms from equations (7) and (8).

Now the energies of such states can be determined from heat capacity measurements since an additional contribution — the so-called Schottky anomaly — occurs from changes in their population with temperature. In order to resolve this contribution the heat capacity of the lattice has to be removed and frequently this proves troublesome. However if the Schottky anomaly occurs at low temperatures the errors involved are considerably reduced. This additional contribution to the heat capacity from  $N$  rare earth ions at temperature  $T$  thermally populating  $(n + 1)$  states of energy  $E_i$  (K) and degeneracy  $g_i$  [7] is given by

$$C_V/R = Z^{-1} \left\{ \sum_{i=0}^n g_i (E_i/T)^2 \exp (-E_i/T) - \right. \\ \left. - Z^{-1} \left[ \sum_{i=0}^n g_i (E_i/T) \exp (-E_i/T) \right]^2 \right\} \quad (9)$$

where  $E_0$  is assumed to be zero and the partition function  $Z$  is given by

$$Z = \sum_{i=0}^n g_i \exp (-E_i/T) \quad (10)$$

The additional entropy associated with the removal of the degeneracy of the entire ground level is

$$\Delta S/R = \ln \left( \sum_{i=0}^n g_i \right) - \ln g_0$$

Frequently the separation of the states is such that it is very instructive to begin the interpretation of the results by con-

sidering the contribution from a two state system. Equation (9) then reduces to

$$C_V/R = (E_1/T)^2 (g_0/g_1) \exp (E_1/T) \\ [1 + (g_0/g_1) \exp (E_1/T)]^{-2} \quad (11)$$

Since the most obvious feature of a Schottky anomaly is its maximum value we would like to draw attention to the frequently neglected use that can be made of this feature, namely that from it  $E_1$  and  $g_1/g_0$  can be deduced immediately. Thus the maximum value ( $C_m$ ) of eq (11) does not depend on  $E_1$  but is a simple function of  $g_1/g_0$  [11] and is given by the relations

$$C_m/R = 4 (g_1/g_0) \exp (E_1/T_m) \\ [\exp (E_1/T_m) - (g_1/g_0)]^{-2} \quad (12)$$

$$E_1/T_m = 2 [\exp (E_1/T_m) + (g_1/g_0)] \\ [\exp (E_1/T_m) - (g_1/g_0)]^{-1} \quad (13)$$

$C_m/R$  and  $E_1/T_m$  are plotted as a function of  $g_1/g_0$  in figure 1.

However if splitting of the states by the crystal field is small the interpretation is less straightforward and some initial consideration of the order of the states predicted by theory provides useful guidance.

In the phases where exchange interaction is small the energies can be determined from equation (4) but in many instances the effects of exchange are important and allowance has to be made for them in the Hamiltonian. Therefore let us consider the extra term needed in the Hamiltonian when there is both an applied magnetic field and exchange interaction.

### 3.2. *The effects of a magnetic field*

Assume that only the lowest level of the multiplet is significantly populated (this is a reasonable assumption for all the phases except  $\text{SmPd}_3$  and  $\text{EuPd}_3$ ) and that the exchange interac-

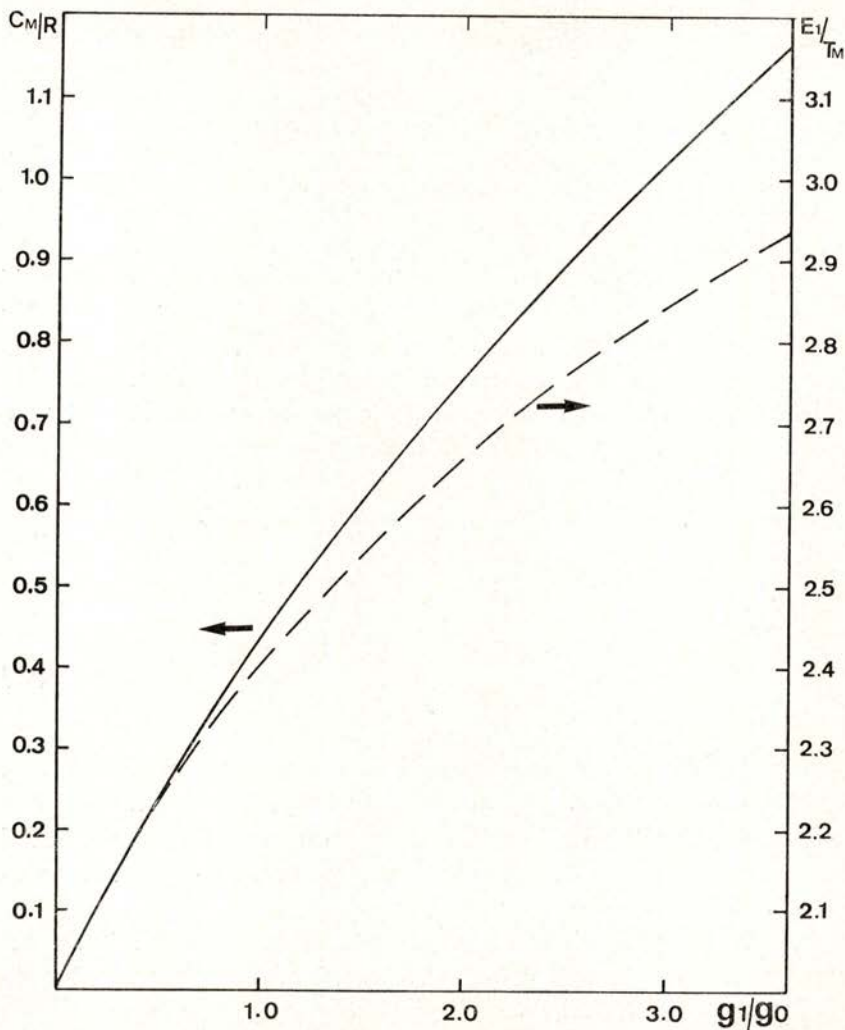


Fig. 1 — Maximum heat capacity/g atom of a two-level system of ions (—) and ratio of the energy separation of the levels ( $E_1$ ) and the temperature of the maximum ( $T_m$ ) (---) as a function of the ratio of the degeneracies of the two levels.

tion acts only on the spin-component of  $J$ . Then the extra term in the Hamiltonian can be written

$$\mathcal{H}_m = \mu_B [(\mathbf{H}_{ex} + \mathbf{H}_a) \cdot 2 \mathbf{S} + \mathbf{H}_a \cdot \mathbf{L}] \quad (14)$$

where  $H_{ex}$  is the exchange field and  $H_a$  is the applied field i.e. the external field corrected for the demagnetizing field. Since the crystal field and magnetic interactions are small compared to the spint-orbit interaction  $\mathcal{H}_m$  can be rewritten

$$\mathcal{H}_m = \mu_B g J \cdot \{ H_a + 2 [(g - 1)/g] H_{ex} \} = \mu_B g J \cdot H \quad (15)$$

where  $g$  is the Landé factor. Thus the exchange interaction need not be treated separately but can be simply added to the applied field.

In order to diagonalize the Hamiltonian modified by this additional term it is simplest if the magnetic field is assumed to be along the axis of quantization. Using equations (2) — (4), solutions can be obtained for the three major symmetry directions. However for a polycrystalline sample all orientations of  $H$  with respect to the crystal axes have to be evaluated and an average obtained. This is not necessary in order to determine the magnetic susceptibility ( $\chi_m$ ) since this is a scalar quantity in a crystal with cubic symmetry and therefore a calculation along any of the crystal axes is sufficient to determine it. However the magnetization does depend on direction and a full calculation is necessary. Since this involves excessive computing time we have been forced to approximate and we have only made calculations in the three principal symmetry directions and obtained an estimate of the polycrystalline magnetization ( $M_p$ ) from their weighted average:

$$M_p = (1/26) [ 6 M < 100 > + 8 M < 111 > + 12 M < 110 > ] \quad (16)$$

In order to make a comparison with the experimental results we assume some values for the crystal field parameters (or  $x$  and  $W$ ) and the magnetic field and diagonalize the Hamiltonian in the 3 principal directions to obtain the energy states and wave functions. Use is then made of these to calculate the heat capacity, entropy, magnetization and susceptibility. Expressions for the heat capacity and entropy have been given above. The expressions used to determine the magnetization and susceptibility are

$$M_z = N \sum_{2J+1} \mu(i) \exp [ - E(i)/T ] / \sum_{2J+1} \exp [ - E(i)/T ] \quad (17)$$

$$\chi_m = N \sum_{2J+1} \{ [W_1(i)^2/T] - 2 W_2(i) \} \exp [-W_0(i)] / \sum_{2J+1} \exp [W_0(i)/T] \quad (18)$$

$$E(i) = W_0(i) + W_1(i) H_Z + W_2(i) H_Z^2$$

$$W_1(i) = \langle \psi_i | g \mu_B J_Z | \psi_i \rangle$$

$$W_2(i) = \sum_{n \neq i} | \langle \psi_n | g \mu_B J_Z | \psi_i \rangle |^2 [E_i - E_n]^{-1}$$

In order to interpret magnetization data it is useful to consider the limiting values of these expressions. At  $T = 0$  K only the ground state is populated, and, neglecting exchange interaction and the temperature-independent contributions from the excited states, its magnetic properties are

$$\mu_{\text{sat}} = \langle \Gamma_s | g \mu_B J_Z | \Gamma_s \rangle \quad (19)$$

$$\mu_{\text{eff}}^2 = 3 \sum_r | \langle \Gamma_r | g \mu_B J_Z | \Gamma_r \rangle |^2 g_0^{-1} \quad (20)$$

where the 'largest' wave function is chosen for  $\Gamma_s$  and the summation for  $\mu_{\text{eff}}^2$  is over all the  $g_0$  states composing the ground state.

Simply by using the known degeneracy of the crystal field states and equations (19) and (20) it can be shown [12] that the following relations hold for  $\mu_{\text{eff}}$ :

$$\mu_{\text{eff}} = \sqrt{2} \mu_{\text{sat}} \quad \text{if } \Gamma_4 \text{ (or } \Gamma_5) \text{ is the lowest state;} \quad (21)$$

$$\mu_{\text{eff}} = \sqrt{3} \mu_{\text{sat}} \quad \text{if } \Gamma_6 \text{ (or } \Gamma_7) \text{ is the lowest state;} \quad (22)$$

$$\sqrt{3/2} \mu_{\text{sat}} < \mu_{\text{eff}} < \sqrt{3} \mu_{\text{sat}} \quad \text{if } \Gamma_8 \text{ is the lowest state.} \quad (23)$$

When  $T \gg$  crystal field splittings, equation (18) becomes Curie's law

$$\chi_m = g^2 J(J+1) / 3T = \mu_{\text{eff}}^2 / 3T \quad (24)$$

Therefore in the absence of exchange the susceptibility obeys Curie's law at high temperatures i.e.  $1/\chi$  is a linear function of  $T$  but departures from the straight line occur as  $T \rightarrow 0$ , as the value of  $\mu_{\text{eff}}^2$  changes. In the case of non-magnetic ground states

the value of  $1/\chi_m$  becomes constant as  $T \rightarrow 0$ , this constant value being determined by the temperature independent contributions from the excited states (see eq. (18)). In the rare earth compounds, where the overall crystal field splittings are  $\sim 200$  K, a plot of  $1/\chi_m$  as a function of  $T$  which only includes data taken over a small temperature interval can be misleading since it frequently appears linear with a positive or negative intercept. This intercept is often taken as an indication of the presence of an exchange interaction. However from the above discussion it is clear that it may simply be associated with temperature dependent effects due to the crystal field.

The effects of exchange interaction can be taken into account using the molecular field approximation,

$$H_{\text{ex}} = \lambda M \quad (25)$$

It is simple to show that when  $M$  is linear in  $H_a$  [13]

$$H_a / M = \chi_{\text{obs}}^{-1} = \chi_m^{-1} - 2 [(g - 1) / g] \lambda \quad (26)$$

where  $\chi_m$  is given by equation (18). Thus the effect of the exchange interaction on the magnetic susceptibility is to increase (or decrease)  $1/\chi_m$  by an amount independent of temperature above the ordering temperature. If  $\chi_m$  satisfies eq (24) we obtain the Curie-Weiss law

$$\chi_{\text{obs}} = \mu_{\text{eff}}^2 / 3 (T - \Theta) \quad (27)$$

where

$$\Theta = (2/3) [(g - 1) / g] \lambda \mu_{\text{eff}}^2 \quad (28)$$

At low temperatures  $M$  is no longer linear in  $H_a$  but shows signs of saturation. This behaviour can be calculated using equations (16) and (17), but some simple comments are helpful. For an isolated crystal field state the saturation moment is seen, from equations (21), (22) and (23), to be independent of the direction of  $\mathbf{H}$  relative to the crystal axes except for  $\Gamma_8$ . In the case of  $\Gamma_8$  the maximum value depends on direction and varies considerably with the wave-functions. For illustration consider

Er<sup>3+</sup> [14]\*; the saturation moment in the three principal directions is given in table 5 (page 84) for the three  $\Gamma_8$  states, for a fourth-degree field only. It will be noticed that the maximum value occurs in either the  $\langle 100 \rangle$  or the  $\langle 111 \rangle$  direction in agreement with the predictions of Trammel [15]. Trammel has shown that if only fourth-order fields are present the easy axis depends on the sign of the anisotropy and can be in either the  $\langle 100 \rangle$  or  $\langle 111 \rangle$  direction. Sixth-order fields have to be present if the  $\langle 110 \rangle$  is the easy direction.

In phases where crystal state splittings are small it is important to consider the mixing of the crystal field states by a magnetic field. For example separation of the first excited state in ErPd<sub>3</sub> is only 2 K from the ground state and energy changes of this magnitude are readily achieved in rare earth phases since a field of 10<sup>4</sup> Oe lowers the energy of a state of magnetic moment  $1 \mu_B$  by 0.675 K. Thus it is possible to have not only strong mixing produced between the states but also actual crossing-over of states. Bleaney [13] in his pioneer paper in this area produced quantitative results for some simple situations such as T = 0 K and field mixing of only the two lowest states. He showed that the maximum possible moment at T = 0 K for the mixed state with **H** in the z direction is given by

$$\mu_{\text{sat}} (\text{max}) = (1/2) g \mu_B \{ a + b + [(a-b)^2 + 4c^2]^{1/2} \} \quad (29)$$

where  $a = \langle \psi_0 | J_z | \psi_0 \rangle$ ,  $b = \langle \psi_1 | J_z | \psi_1 \rangle$ ,  $c = \langle \psi_1 | J_z | \psi_0 \rangle$ .

As an example, equation (29) is very useful in considering the maximum effect of an excited state on a non-magnetic ground state.

Finally although we have not made measurements of heat capacity in an applied field the results obtained in zero field are affected by the exchange field. This will produce a large magnetic contribution to the heat capacity at the ordering temperature which will take the typical  $\lambda$  - form.

---

(\*) Many of the results of this paper given in their table 2 need correcting as a spectroscopic stability check will indicate.

The additional heat capacity is associated with a change in separation and loss of degeneracy in the crystal field states. The detailed behaviour depends on the approximation used for describing the exchange interaction and will not be calculated in this paper. However if the ground state has a degeneracy  $g_0$  there will be an associated entropy change

$$\Delta S / R = \ln g_0 \quad (30)$$

#### 4 — HEAT CAPACITY RESULTS \*

##### 4.1. LaPd<sub>3</sub>

The heat capacity of a 9.454 g sample of LaPd<sub>3</sub> (MW = 458.1) was measured from 1.6 to 6.9 K and the results are given in figure 2 where  $C_V/RT$  is plotted versus  $T^2$ . It can be seen imme-

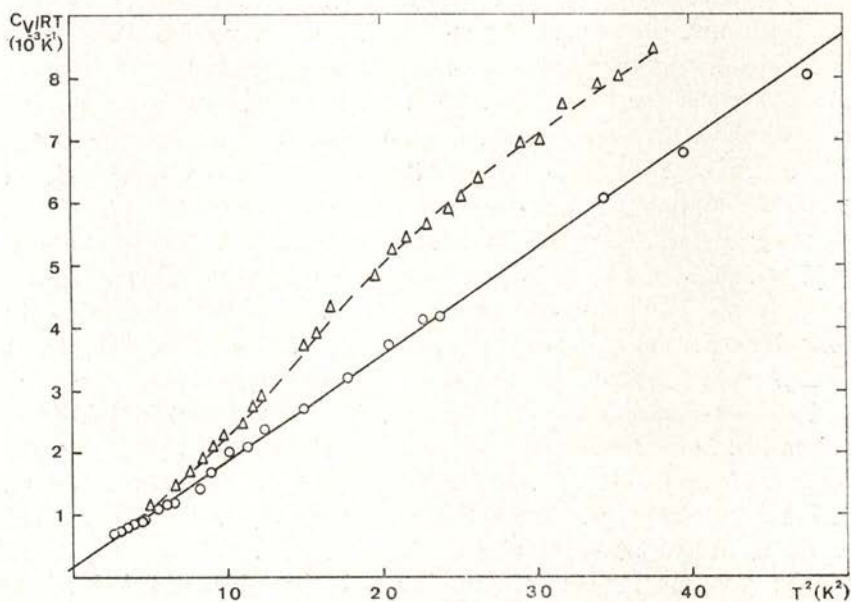


Fig. 2 — Heat capacity/g molecule of LaPd<sub>3</sub>: o — this investigation; Δ — Hutchens et al. [4]

(\*) A previous account of the heat capacity results has been published in [16], [17].

diately that the data are described by equation (1) with  $\gamma = 0.33 \pm 0.02$  mJ/(K<sup>2</sup>. g atom) and  $\Theta_D = 171 \pm 1$  K. Hutchens *et al* [18] have also measured the heat capacity of a LaPd<sub>3</sub> sample, and their data are also plotted in figure 2. The agreement between the two sets of data is rather poor although there is coincidence at about 2 K. It is physically impossible to describe the data of Hutchens *et al* [4] by equation (1) since such a fit for the lowest temperature results would lead to a negative value for  $\gamma$ . Hutchens *et al* [4] overcome this difficulty by the introduction into the specific heat of a contribution from a postulated conduction electron spin fluctuation interaction [19]. The possibility of such a contribution will be considered in the discussion of the results.

#### 4.2. PrPd<sub>3</sub>

The heat capacity of a 17.975 g sample of PrPd<sub>3</sub> (MW = 460.1) has been measured from 0.35 to 10.7 K and the results\* are given in figure 3, together with the heat capacity of LaPd<sub>3</sub>. There are three obvious features: (i) a  $\lambda$  - type maximum with  $C_v/R \sim 0.7$  at 0.6 K which suggests the occurrence of magnetic ordering, (ii) a broad maximum at 2 K with  $C_v/R \sim 0.3$  which is a Schottky anomaly from the two 4f electrons of Pr<sup>3+</sup>, (iii) the crossing of the heat capacity curves of LaPd<sub>3</sub> and PrPd<sub>3</sub> at about 9 K which indicates a larger Debye temperature for the latter. In order to calculate the observed behaviour we have first to consider the crystal field states of Pr<sup>3+</sup>. The *ab initio* point charge model predicts a predominant fourth-degree field (table 1) and the energies of the 4 states involved are given in table 2a, column 3. Note firstly that the ground state is a triplet state  $\Gamma_5$  with a doublet state  $\Gamma_3$  at 51 K. If such a configuration existed in PrPd<sub>3</sub> it would produce a Schottky anomaly with a maximum of  $C_v/K$  of 0.3 at  $\sim 22$  K (see figure 1) *i.e.* outside the range of the present measurements. Instead the observed behaviour suggests that the separation of the two lowest states is  $\sim 5$  K, rather than 51 K, and that the threefold degeneracy of the  $\Gamma_5$

---

(\*) In order to plot the results for PrPd<sub>3</sub> a correction was required since the magnetic measurements (Section 5.1) showed that the sample only contained  $22.0 \pm 0.5\%$  Pr.

TABLE 1

	a (Å)	$\langle r^4 \rangle$ (a.u.) <sup>4</sup>	$\langle r^6 \rangle$ (a.u.) <sup>6</sup>	x	W (K)	$A_4 \langle r^4 \rangle$ (K)	$A_6 \langle r^6 \rangle$ (K)
Pr	4.129	2.822	15.726	-0.983	-1.81	-40.5	-0.40
Tb	4.068	1.419	5.688	-0.992	0.162	-21.9	-0.16
Er	4.045	1.126	3.978	0.935	-0.051	-17.9	-0.12
Yb	4.027	0.960	3.104	-0.909	-1.64	-15.6	-0.09
Nd	4.118	2.401	12.396	0.952	0.6407	-34.9	-0.32
Dy	4.061	1.322	5.102	-0.972	-0.0753	-20.6	-0.15
Ho	4.054	1.224*	4.540*	0.9429	0.0406	-19.2	-0.13
Tm	4.039	1.043*	3.541*	-0.9735	0.1721	-17.1	-0.11

\* Interpolated values.

TABLE 2 (a) — The energies of the crystal field states of  $Pr^{3+}$  derived from the ground level  $^3H_4$

State	Degeneracy	Calculated Energy (K) Schemes		
		(i) Point charge model	(ii) Best experimental fit	(iii) A possible fit
$\Gamma_5$	3	0	0	1.52
$\Gamma_3$	2	51	5.0	0
$\Gamma_4$	3	71	100	4.02
$\Gamma_1$	1	98	(233)	12.54

state is removed at 0.6 K. However it is possible to fit the peak value at 0.6 K with a Schottky contribution assuming a 2-fold degenerate ground state and 3-fold level at 1.50 K (see figure 1). However using eq. (9) and the energy levels of column 5 table 2a it can be seen (figure 3) that the overall contribution between 0.6 and 3 K is much too large when a fit to the broad maximum at 2 K is also attempted. Thus the  $\lambda$  - type maximum is undoubtedly associated with a magnetic transition in which the degeneracy of the ground state is removed.

This broad interpretation is unaffected by estimates of the lattice and electronic specific heats but in order to obtain a

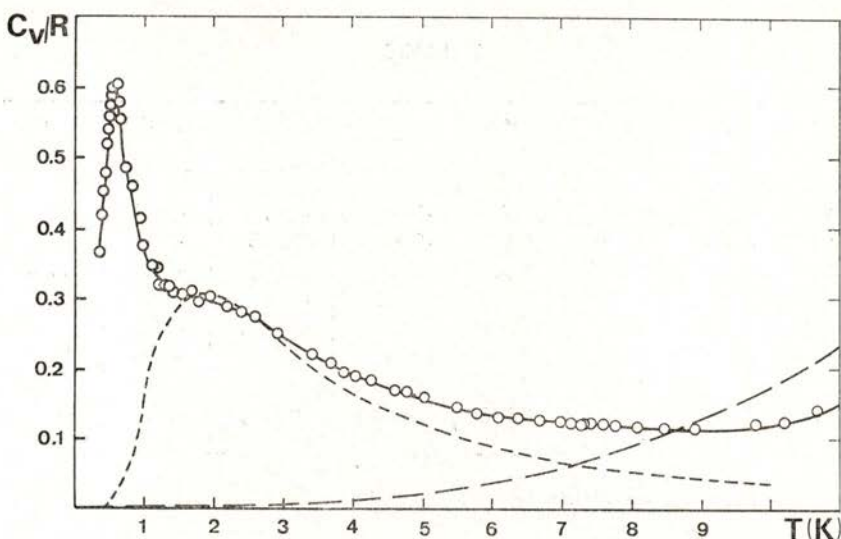


Fig. 3 — Heat capacity/g molecule of  $\text{PrPd}_3$  as a function of temperature: o experimental results; ---- theoretical curve for energy scheme (ii) of table 2a; —  $\text{LaPd}_3$ .

detailed fit above 4 K these terms must be considered. If we ignored their contribution entirely a second excited state at  $\sim 60$  K would fit the observed value at 10.5 K which therefore sets a lower limit on the energy of this state. Now the lattice and the electronic contributions are represented by equation (1) and we anticipated that since the two compounds  $\text{LaPd}_3$  and  $\text{PrPd}_3$  have similar metallic lattices and, probably, similar melting points, the lattice (from the Lindemann equation) and conduction electron terms of  $\text{PrPd}_3$  would be very similar to those of  $\text{LaPd}_3$  (given in 4.1). The results above 9 K (figure 3) show that this is clearly untrue and we have assumed instead that although the electronic contribution is unchanged and given by equation (1) the lattice contribution is halved. The specific heat at 10.5 K can now be fitted with a second excited state  $\sim 100$  K. The calculated curve which gives the best experimental fit to the overall data is shown in figure 3. It is derived from equation (9) using the energy levels of column 4, table 2a. The fit is sensitive to the choice of energy of  $\Gamma_3$  and acceptable fits are obtained for  $\Gamma_3 = 5.0 \pm 0.5$  K,  $\Gamma_4 = 100 \pm 10$  K. When

$\Gamma_3 = 5.5$  K the theoretical curve slightly exceeds the experimental points above about 3 K. Our choice of 5.0 K permits the possibility of a short range contribution up to about 9 K. In fact the error in  $\Gamma_3$  ( $\pm 0.5$  K) mainly lies in trying to estimate this contribution whereas the error in  $\Gamma_4$  ( $\pm 10$  K) lies in the assumption made about the lattice specific heat. Further light on the interpretation can be made by considering the entropy variation up to 10.7 K. The observed entropy variation between 0.35 and 10.7 K is  $S/R = 1.142 \pm 0.020$ .

The calculated entropy variation associated with the best theoretical fit is  $0.523 \pm 0.010$ . The difference represents the magnetic contribution above 0.35 K. In order to calculate the total magnetic contribution it is necessary to estimate the entropy change below 0.35 K. The temperature dependence of the heat capacity is unknown but the entropy at 0.35 K is 0.139 for a  $T^3$  dependence and 0.415 for a  $T$  dependence. We will take  $0.27 \pm 0.1$  as a reasonable estimate and therefore the total entropy change associated with the magnetic ordering up to 11 K is  $0.89 \pm 0.1$ .

This magnetic entropy is significantly smaller than  $\ln 3$  (1.099) even though the temperature interval considered should have included most of the contribution from short range ordering above the ordering temperature [20]. This discrepancy could be explained if the praseodymium content was 16.5% instead of 22% but this difference far exceeds experimental error. We believe that the discrepancy occurs because the magnetic ordering commencing at 0.6 K is incomplete. The lack of entropy does not indicate, as discussed above, that the anomaly is a non-magnetic one.

The energy values deduced above to fit the specific heat data can be used to determine the fourth and sixth degree terms. An examination of the diagram of energy states (figure 4 (a) LLW) for  $\text{Pr}^{3+}$  shows that  $\Gamma_5$  and  $\Gamma_3$  cross at  $x \sim -0.74$ . The observed energy values show that  $x$  has to be less than but close to this value. In fact knowing the energy (and degeneracies) of the first two excited states with respect to the ground state,  $W$  and  $x$  (or  $A_4 \langle r^4 \rangle$  and  $A_6 \langle r^6 \rangle$ , or  $Z_1$  and  $Z_2$ ) can be determined immediately from the solution of two simple simultaneous equations. The results are given in table 2b. It can be seen that the simple point charge model estimate of

TABLE 2 (b) — The parameters associated with the crystal field states of Pr<sup>3+</sup>

	x	w	A <sub>4</sub> <r <sup>4</sup> > (K)	A <sub>6</sub> <r <sup>6</sup> > (K)	Z <sub>1</sub>	Z <sub>2</sub>
(i)	-0.983	-1.81	-40.5	-0.40	0	3
(ii)	-0.747	-4.20	-71.1	-13.8	-2.92	-2.99
(iii)	-0.645	-0.145	-2.12	-0.66	-0.147	-0.259

both crystal field terms was low and that in particular the sixth degree term is large and significant in PrPd<sub>3</sub>, being about 20 % of the fourth degree term. The values obtained for Z<sub>1</sub> and Z<sub>2</sub> do not appear to have a simple explanation. In conclusion, this analysis of the heat capacity results of PrPd<sub>3</sub> has produced the crystal field parameters A<sub>4</sub> <r<sup>4</sup>> = - 71 ± 10 K and A<sub>6</sub> <r<sup>6</sup>> = - 14 ± 2 K, where the errors correspond to the limit of acceptable fits. The errors are primarily associated with the uncertainty in the lattice contribution and if the data had been taken to 20 K the above errors would have been reduced considerably, and become comparable to those obtained using neutron scattering techniques [21]. Thus we are able to refute the conclusion [21] that «only direct spectroscopic measurements can yield parameters of sufficient accuracy to be of any use in evaluating models for the microscopic origins of crystal fields in metals». In fact the proper conclusion is that the determination of crystal field parameters of sufficient accuracy depends on whether the energy levels that are affecting the observations are associated with a wide or narrow range of crystal field values. It seems evident that, since the variation of the energy levels of the various rare earths as a function of the two crystal field parameters is somewhat complicated, broad sweeping conclusions of the above kind are always liable to be wrong.

#### 4.3. TbPd<sub>3</sub>

The heat capacity of a 5.207 g sample of TbPd<sub>3</sub> (MW = 478.1) has been measured from 2.1 to 8.6 K and the results (\*) are given in

(\*) The alloy composition was checked using standard chemical techniques and agreed (± 0.48 %) with the nominal composition.

figure 4 where  $C_v/R$  is plotted versus temperature. The results have been plotted on two scales, which differ by a factor of 10, in order to show the features fully. The heat capacity shows a typical  $\lambda$ -anomaly with a maximum value of  $C_v/R$  of  $\sim 7.0$  at

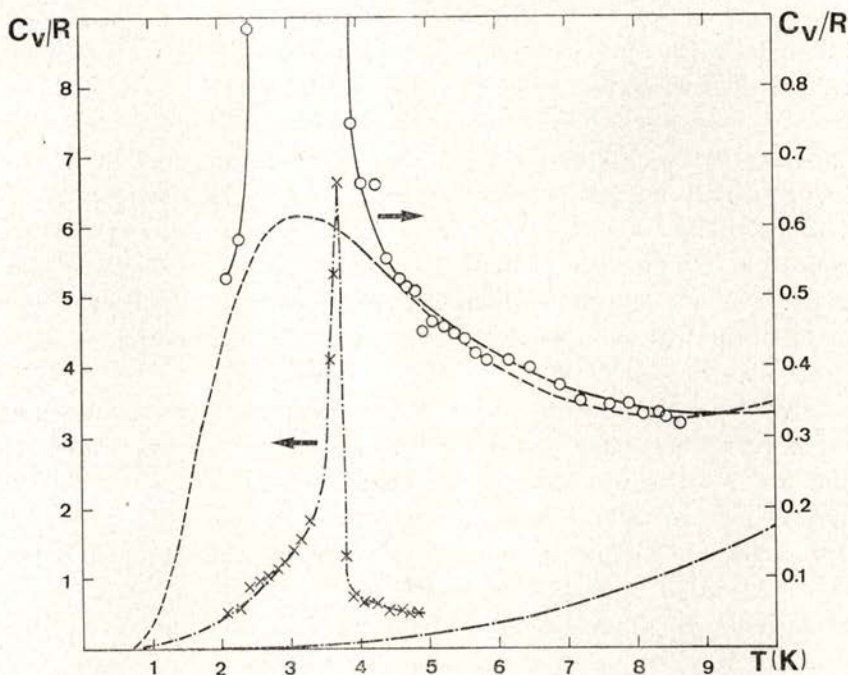


Fig. 4 — Heat capacity/g molecule of  $TbPd_3$  as a function of temperature. The dashed curves in the figure (except that of  $LaPd_3$ ) represent theoretical fits: — · — a  $T^3$  curve fitted at 2.5 K; - - - 0,8,60 + lattice heat capacity of  $LaPd_3$ ; — — — 0,8,33 + lattice heat capacity deduced for  $PrPd_3$ ; — · — the heat capacity of  $LaPd_3$ . The ordering temperature is 3.75 K

a temperature of 3.75 K indicating that magnetic ordering occurs at this temperature. In addition, the heat capacity up to 8.6 K is always greater than that of  $LaPd_3$  (figure 4) indicating either that above 3.75 K there is a continuing contribution from the magnetic interaction or that there is a crystal field contribution also occurring. If the latter situation applies to  $TbPd_3$ , then, unlike  $PrPd_3$ , where the magnetic and Schottky anomalies were almost resolved, in  $TbPd_3$  there is considerable overlap. Despite this

greater complexity a consideration of the entropy as a function of temperature, the heat capacity above the  $\lambda$ -point and the predictions of the point charge model lead to a reasonable interpretation of the data.

As a consequence of experimental difficulties during the measurement of TbPd<sub>3</sub>, the heat capacity results commence at 2.1 K and thus an estimate of the entropy below this temperature is necessary. This has been obtained by assuming no further anomalies occur below the  $\lambda$ -point and that the heat capacity below 2.5 obeys a  $T^3$  law. We believe that the error involved in these assumptions is small and is  $\Delta (S/R) \sim \pm 0.05$ . The calculated entropy at the ordering temperature (3.75 K) is  $1.10 \pm 0.10$  and the values obtained between 4 and 9 K are given in table 3a. It is immediately evident that the entropy at the ordering temperature is close to  $\ln 3$  (1.099) and at 9 K lies between  $\ln 4$  (1.386) and  $\ln 5$  (1.609).

We have not attempted to fit the heat capacity data below the  $\lambda$ -point but have considered its behaviour between 4.5 K and 8.6 K. The *ab initio* point charge model ( $Z_1 = 0$ ,  $Z_2 = 3$ ) predicts, as in PrPd<sub>3</sub>, a predominant fourth degree term (table 1). The resulting energies of the 6 crystal field states obtained from the  ${}^7F_6$  ground level of Tb<sup>3+</sup> are given in table 3b, column 5. The predicted ground state is the non-magnetic doublet  $\Gamma_3$  with a triplet state  $\Gamma_5^{(1)}$  at 1.9 K and a singlet state  $\Gamma_2$  at 7.9 K. The calculated heat capacity from such a configuration bears no resemblance either to the entropy or the heat capacity data above 4.5 K. We have therefore calculated the change in heat

TABLE 3 (a) — The entropy S/R of TbPd<sub>3</sub>

T(K)	Observed	Observed—ln2	(i)	(ii)
4	$1.15 \pm 0.10$	$0.45 \pm 0.10$	0.527	0.526
5	1.28	0.58	0.645	0.644
6	1.36	0.66	0.725	0.727
7	1.42	0.73	0.782	0.787
8	1.47	0.77	0.827	0.835
9	1.50	0.81	0.866	0.874

TABLE 3 (b) — The energies of the crystal field states of Tb<sup>3+</sup>, ground level <sup>7</sup>F<sub>6</sub>

State	Degeneracy	Observed Energy (K)		Calculated Energy (K)
		(i)	(ii)	(iii)
Γ <sub>3</sub>	2	0	0	0
Γ <sub>5</sub> <sup>(1)</sup>	3	8	8	1.9
Γ <sub>2</sub>	1	60	33	7.9
Γ <sub>5</sub> <sup>(2)</sup>	3	—	(116)	27.5
Γ <sub>4</sub>	3	—	(139)	32.9
Γ <sub>1</sub>	1	—	(159)	37.6

capacity associated with these 3 states upon varying their separation and order. We find that the heat capacity results are sensitive both to the separation and order of the two lowest states and that, irrespective of any assumptions about the lattice specific heat, a good fit is possible only if the ground state is Γ<sub>3</sub> and the energy of Γ<sub>5</sub><sup>(1)</sup> is 8.0 ± 0.5 K. On the other hand, the calculated energy of the Γ<sub>2</sub> state does depend on the choice made for the lattice heat capacity. If we assume that this is the same as LaPd<sub>3</sub> a good fit to experimental values is obtained (see figure 4) if the energy of Γ<sub>2</sub> is 60 ± 10 K, whereas if the lattice heat capacity adopted for PrPd<sub>3</sub> is assumed an equally good fit can be achieved (see figure 4) if the energy of Γ<sub>2</sub> is 33 ± 5 K.

The entropy values have also been calculated for these two cases and are given in table 3a. These values have to be compared with the observed values less the magnetic entropy associated with the Γ<sub>3</sub> ground state (ln 2) which are also given in table 3a. The agreement is good and in fact improves when the separation of Γ<sub>3</sub> and Γ<sub>5</sub><sup>(1)</sup> is taken as 8.5 K. We think that, in spite of the assumptions necessary to compare calculation with experiment, the results show clearly that the ground state cannot be Γ<sub>5</sub><sup>(1)</sup>, with short range order contributions above the ordering temperature, nor could we find a satisfactory configuration of states that would produce a reasonable fit with this ground state. Instead our analysis shows that the ground state

is  $\Gamma_3$  and that if we ignore short range order effects above the ordering temperatures, then the first excited state is  $\Gamma_5^{(1)}$  at 8 K and that the second excited state  $\Gamma_2$  lies at 33 K or 60 K (or perhaps an intermediate value) depending on the magnitude of the lattice heat capacity. These energy values deduced to fit the heat capacity data can be used to determine the fourth- and sixth-degree terms. An examination of the energy diagram for TbPd<sub>3</sub> (figure 6b in Lea, Leask and Wolf [10]) shows that the separation of  $\Gamma_3$  and  $\Gamma_5^{(1)}$  only varies slightly between  $x = -1$  and  $-0.7$  and that these states cross at  $x \sim -0.5$ , whereas the energy separation of  $\Gamma_2$  and  $\Gamma_3$  varies linearly with  $x$ . Consequently, we can fit a second excited state at  $\sim 33$  K with a value of  $x$  close to  $-1.0$ , whereas if  $\Gamma_2$  is at 60 K a value of  $x \sim -0.75$  is required; the corresponding values of the crystal field parameters,  $W$  and  $Z_1$

TABLE 3 (c)

	$x$	$W$	$A_4 \langle r^4 \rangle$	$A_6 \langle r^6 \rangle$	$Z_1$	$Z_2$
(i)	-0.75	0.582	-59.5	-18.0	-9.58	-18.95
(ii)	-0.99	0.682	-92.0	-0.84	-0.09	12.3
(iii)	-0.992	0.162	-21.9	-0.160	0	3

- (i) lattice heat capacity based on the LaPd<sub>3</sub> results, energy states 0,8,60.  
 (ii) lattice heat capacity based on the PrPd<sub>3</sub> results, energy states 0,8,33.

and  $Z_2$  are given in table 3c. For energy scheme (ii) we allowed  $x$  to take the point charge value and the calculated value of  $W$  is roughly 4 times greater than the point charge value. Energy scheme (i) involves a large sixth degree term and the values of  $A_4 \langle r^4 \rangle$  and  $A_6 \langle r^6 \rangle$  are very similar to those obtained for PrPd<sub>3</sub> (table 2b). The two proposed energy schemes correspond to very different values of  $x$  namely  $x = -0.99$  and  $-0.75$ . The corresponding crystal field parameters,  $W$  and  $Z_1$  and  $Z_2$  are given in table 3c. Inelastic neutron scattering results on TbPd<sub>3</sub> [22] exhibit a transition peak at  $\sim 6$  meV. This might well suggest that the energy of  $\Gamma_2$  is indeed  $\sim 60$  K.

Finally, the effects of the exchange energy on the crystal field states should be considered. The observed entropy at the ordering temperature is close to  $\ln 3$  and our analysis has shown that this corresponds to the removal of the twofold degeneracy of the  $\Gamma_3$  state and the depopulation of the excited states below 3.75 K. We have also obtained good agreement above 3.8 K by assuming that the short range ordering is small and this is perhaps not surprising since the magnetism of the  $\Gamma_3$  ground state depends on the presence of an exchange field which, at least in the molecular field model disappears at the ordering temperature. In order to determine the effect of an exchange field we have calculated energies of the crystal field states as a function of magnetic field and have found that the  $\Gamma_3$  and  $\Gamma_5^{(1)}$  states do not cross for fields up to 200 kOe. Second order perturbation theory shows that  $\Gamma_3$  magnetizes in second order because of the different mixing terms in the  $\langle 100 \rangle$  direction, so that the state which mixes with  $\Gamma_5^{(1)}$  falls faster than the state mixing with  $\Gamma_4$ . However in the  $\langle 111 \rangle$  direction the degeneracy of the  $\Gamma_3$  state is not removed in second order and therefore it seems likely [15] that ordering will occur in the  $\langle 100 \rangle$  direction. Thus  $\text{TbPd}_3$  is an example of a system which orders in a non-magnetic ground state by exchange induced mixing with higher states.

#### 4.4. $\text{ErPd}_3$

The heat capacity of a 1.700 g sample of  $\text{ErPd}_3$  ( $MW = 486.46$ ) has been measured from 0.2 to 0.9 K and the results are shown in figure 5 where  $C_v/R$  is plotted as a function of temperature. Unfortunately, the experimental results are over a brief temperature interval and therefore the analysis we can carry out is somewhat restricted. However a Schottky anomaly with a maximum at about 0.75 K with  $C_v/R \sim 0.74$  is clearly visible and it is evident that magnetic ordering does not occur in  $\text{ErPd}_3$  above 0.2 K.

$\text{ErPd}_3$  is a system in which magnetic interactions are clearly unimportant and therefore we would anticipate good agreement between the observed data and calculations based on the crystal field energy states. Agreement should be particularly good below

1 K since there is an almost negligible contribution from the lattice and electronic terms.

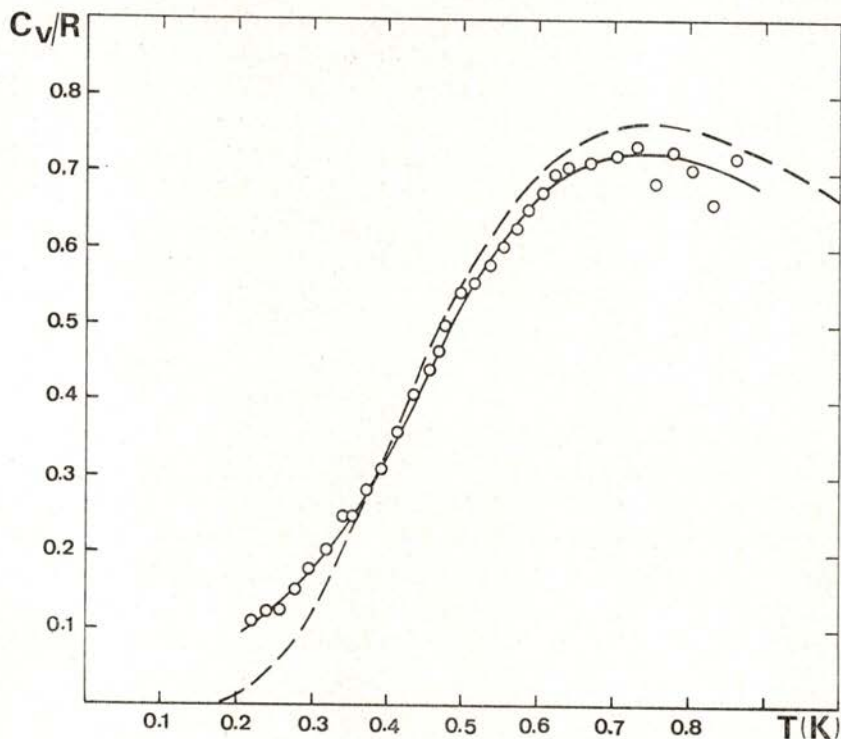


Fig. 5 — Heat capacity / g molecule of  $\text{ErPd}_3$  as a function of temperature. The dashed curve is derived from equation (8) using  $g_1 / g_0 = 2$  and  $E_1 = 2.0$  K.

In the case of  $\text{Er}^{3+}$  the ground level is  $^4J_{15/2}$  and the ab initio point charge model predicts that this level will split into 5 states with the degeneracies and energies given in table 4a. Thus the ground state is the magnetic doublet  $\Gamma_6$  with the four-fold degenerate  $\Gamma_8^{(3)}$  state at 0.7 K, and the two-fold degenerate state  $\Gamma_7$  at 14.1 K. The specific heat data only gives information about the two lowest states. From figure 1 using  $g_1/g_0 = 2$  we anticipate that  $C_m/R = 0.76$  and  $E_1/T_m = 2.66$ . Since  $T_m = 0.75$  K this corresponds to the  $\Gamma_8^{(3)}$  state at 2.0 K. The calculated curve for this energy separation is shown in figure 5 and the agreement is reasonable. The extra specific heat below 0.4 K is probably

TABLE 4 (a) — The energies of the crystal field states of  $\text{Er}^{3+}$

State	Degeneracy	Observed Energy (K)	Calculated Energy (K)				
			(i)	(ii)	(iii)	(iv)	(v)
$\Gamma_6$	2	0	0	0	0	0	0
$\Gamma_8^{(3)}$	4	2	0.7	2.0	2.0	2.0	2.0
$\Gamma_7$	2		14.1	34.4	59.9	23.0	33.4
$\Gamma_8^{(2)}$	4		17.8	44.7	72.9	31.4	43.0
$\Gamma_8^{(1)}$	4		22.7	58.0	93.2	39.8	54.8

ground level  $^4J_{15/2}$   $x = 0.935$   $W = -0.051$  K

due to short range order effects suggesting that ordering occurs below 0.2 K. The observed specific heat at 0.7-0.9 K is somewhat lower than theory but the difference may well be experimental since the results obtained showed considerable scatter. Unfortunately the data are insufficient to enable us to determine the energy of the  $\Gamma_7$  state. However the results clearly show that  $x \sim 0.85$  since below this value the states  $\Gamma_8^{(3)}$  and  $\Gamma_6$  cross [10]. Such a crossing has not occurred since the value of  $C_m/R$  would have been only 0.26 (see figure 1) for  $g_1/g_0 = 0.5$ .

Since the separation of  $\Gamma_6$  and  $\Gamma_8^{(3)}$  is 2.0 K for a given value of  $x$  between 1.0 and 0.85 the corresponding value of  $W$  can be calculated using the variation of energy of these states given by LLW. The corresponding values of  $A_4 \langle r^4 \rangle$  and  $A_6 \langle r^6 \rangle$

TABLE 4 (b)

	$x$	$W$	$A_4 \langle r^4 \rangle$	$A_6 \langle r^6 \rangle$
(i) *	0.935	-0.051	-17.9	-0.12
(ii)	0.935	-0.121	-42.5	-0.27
(iii)	0.90	-0.190	-64.2	-0.662
(iv)	1.0	-0.072	-27.2	0
(v)	0.95	-0.105	-37.4	-0.182

\* point charge model.

can then be determined from eqs (7) and (8). In table 4b these pairs of values are given for  $x = 1.0, 0.95, 0.935$  and  $0.90$ . The effect of decreasing  $x$  is to increase the separation of the higher levels and the total splitting changes from  $E = 40$  K for  $x = 1.0$  to  $E = 93$  K for  $x = 0.90$ .

## 5 — MAGNETIZATION RESULTS

### 5.1. *PrPd<sub>3</sub>*

The magnetization of a 68.1 sphere of *PrPd<sub>3</sub>* has been measured from 1.2 to 50 K in magnetic fields varying from 2 to 42 kOe. The inverse of the observed magnetic susceptibility as a function of temperature is shown in figure 6. The results lie on a curve which does not pass through the origin and suggest the presence of an antiferromagnetic interaction.

The ground level of *PrPd<sub>3</sub>* is  $^3H_4$ . Specific heat measurements (4.2) have shown that crystal field effects are important, that the ground state is  $\Gamma_8$  and the first excited state is  $\Gamma_3$  at 5.0 K and that *PrPd<sub>3</sub>* orders magnetically at 0.6 K. Using the crystal field parameters of table 2b line (ii) the magnetic susceptibility has been calculated using eq (18) and its inverse is shown as a function of temperature in figure 6. For comparison purposes the free ion behaviour of the ground level is also shown. The difference between the observed behaviour and calculated behaviour is due to the exchange interaction present which should produce a displacement independent of  $T$  (eq (2)). Such behaviour is not observed experimentally as shown in the plot (figure 6)

TABLE 5 — The saturation moment ( $\mu_B$ ) in the three principal directions for isolated  $\Gamma_8$  states of  $Er^{3+}$  in a fourth-degree crystal field

State	$\langle 100 \rangle$	$\langle 110 \rangle$	$\langle 111 \rangle$
$\Gamma_8^{(1)}$	5.50	6.23	6.40
$\Gamma_8^{(2)}$	4.78	4.92	4.96
$\Gamma_8^{(3)}$	5.67	5.13	4.84

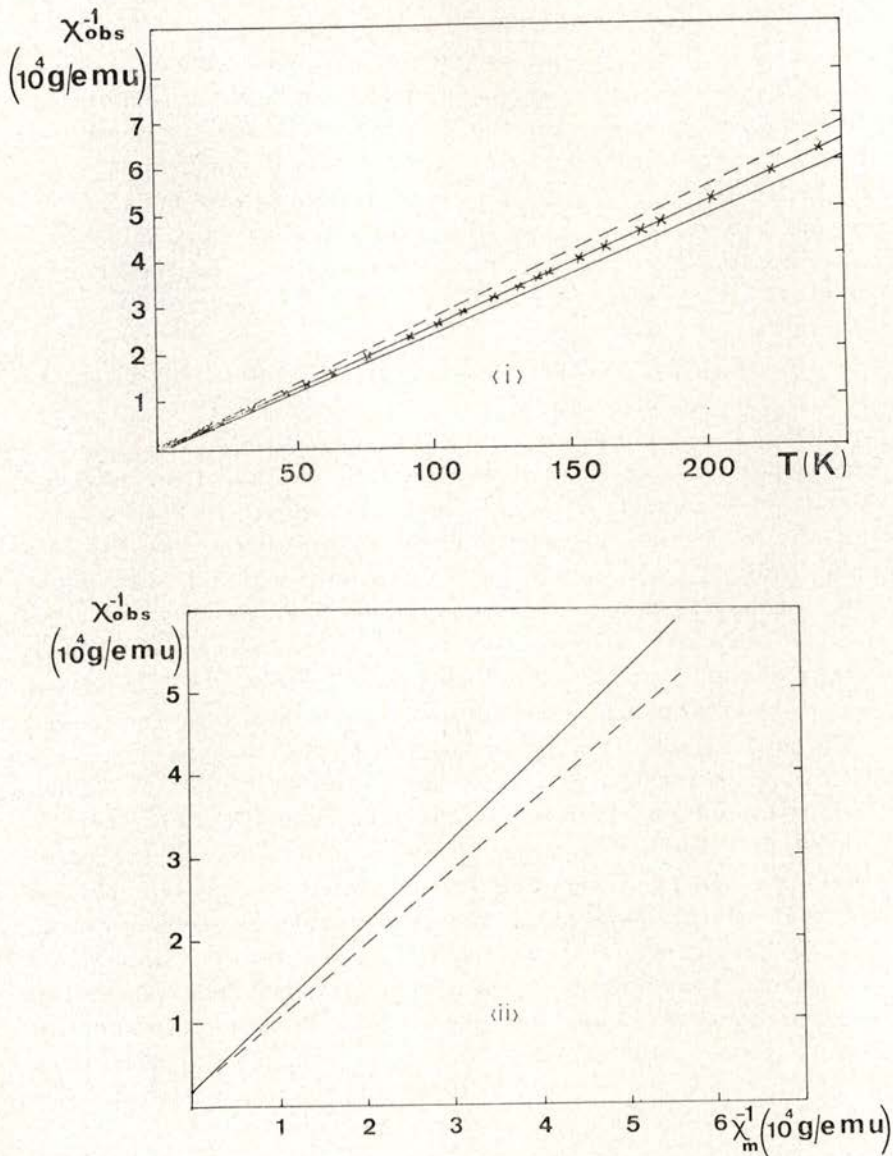


Fig. 6 — (i) The inverse magnetic susceptibility of  $\text{PrPd}_3$  as a function of temperature: x observed results; — — free ion behaviour; — crystal field behaviour. (ii) The inverse magnetic susceptibility of  $\text{PrPd}_3$ ,  $\chi_{\text{obs}}^{-1}$  as a function of the calculated value  $\chi_m^{-1}$ : — observed results; — — slope for 25%  $\text{Pr}^{3+}$  ions / mole.

of the inverse of the observed susceptibility  $(\chi_{\text{obs}})^{-1}$  as a function of the inverse of the calculated susceptibility  $(\chi_{\text{m}})^{-1}$ : If the sample contained 25 % of praseodymium the observed points would lie on the interrupted line instead of the line drawn through them. It is simple to show that the ratio of the slopes of these two lines gives the actual praseodymium content of the sample which is  $22.0 \pm 0.5$  %. The specific heat results given in 4.2 were normalized to 25 % using this value as are the subsequent magnetization results. In addition the value of  $\lambda$  can be deduced from figure 6 using eq (26) and  $g = 0.8$ ; we find  $\lambda = 9.0$  g mole/emu.

The magnetic moment/Pr atom, obtained after correcting the results for the diamagnetism of the matrix ( $-0.15$  emu/g [2]), of PrPd<sub>3</sub> at 4.2 and 1.2 K is shown in figure 7 as a function of the applied magnetic field  $H_a$ , ie the external field less the demagnetizing field. It can be seen that up to 42 kOe at both 1.2 and 4.2 K the magnetic moment varies almost linearly with field, and shows none of the saturation behaviour that might have been anticipated. The theoretical behaviour of the magnetization calculated as indicated in 3.2 using the best fit crystal field parameters of table 2b is shown in figure 7 at 4.2 and 1.2 K for the three principal crystal directions and their average, derived from equation (16). The ground state of PrPd<sub>3</sub> is  $\Gamma_5$  which has a saturation moment of  $2\mu_B$  in isolation. In the  $\langle 100 \rangle$  direction this is approximately true in PrPd<sub>3</sub> (see figure 7) since there is no mixing with the  $\Gamma_3$  state. However the mixing in the other directions causes a significant dependence of the moment on direction above about  $1\mu_B$ . This effect is unimportant in the analysis of our magnetization data since our results, summarised in table 6, are limited to moments less than this value. The discrepancy between the theoretical curves and the experimental results is due to the exchange field which can be evaluated from eq. (15). Using the molecular field approximation and eq (25), values of  $\lambda$  of 10.00 and 11.6 g atom/emu at 4.2 and 1.2 K respectively have been deduced from the data in figure 7. These values are significantly greater than the value deduced from the susceptibility results and suggest that a breakdown of the molecular field approximation occurs as the ordering temperature of 0.6 K is approached. If we use eq. (28) to determine  $\Theta$  from these values of  $\lambda$  we obtain  $\Theta \sim -5$  K, so that  $\Theta$  is an order of magnitude

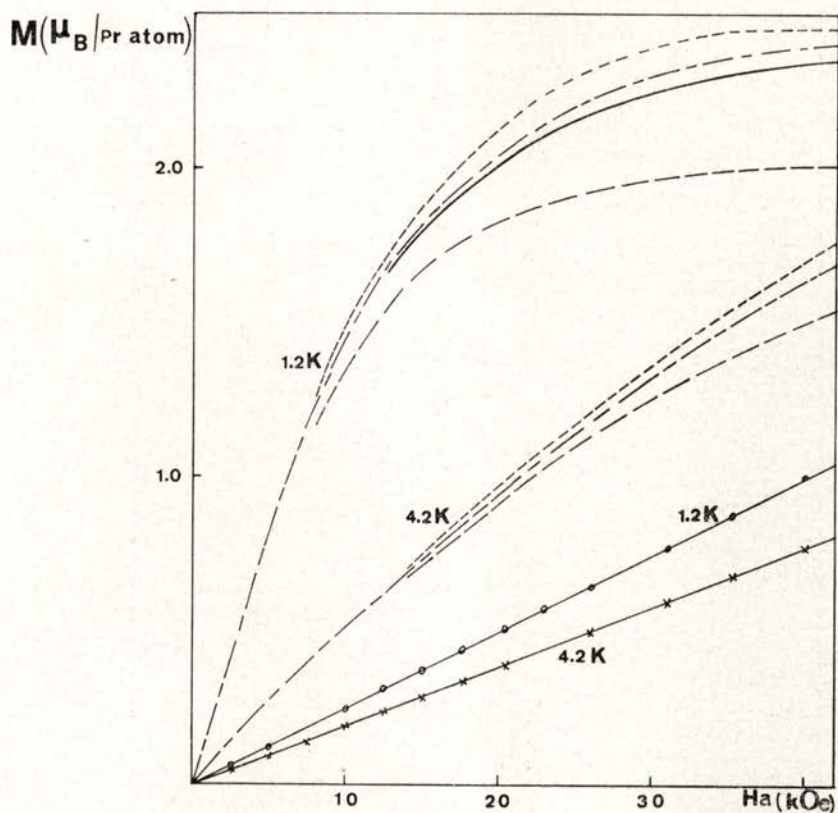


Fig. 7 — The magnetic moment / Pr atom ( $\mu_B$ ) of  $\text{PrPd}_3$  as a function of applied field,  $H_a$ : x (4.2 K), o (1.2 K). The calculated values of  $M_{100}$  (—);  $M_{110}$  (- - -);  $M_{111}$  (- · -) and  $M_p$  (—) at 4.2 K and 1.2 K are also shown. At 4.2 K  $M_p$  (not represented) virtually coincides with  $M_{110}$ .

greater than the ordering temperature. It is possible to account for such a ratio using molecular field arguments. If the ordering was type 1, ie antiferromagnetic chains, the nearest neighbour interaction would be  $\sim 0.36$  K and the nnn interaction  $\sim 0.13$  K whereas if the ordering was type 3 ie ferromagnetic planes, both interactions would be  $\sim 0.21$  K. Type 2 ordering is excluded.

A previous sample of  $\text{PrPd}_3$  [2] containing more than 25 % Pr, since its  $\mu_{\text{eff}}$  above 50 K was greater than the free ion value, was observed to have a value of  $\theta = 0$  K. This suggests that the

TABLE 6

Compound	Ground State	$\mu_{\text{eff}}$ ( $\mu_B$ )	$\mu_{\text{sat}}$ ( $\mu_B$ )	Excited State	$\mu_{\text{eff}}$ ( $\mu_B$ )	$\mu_{\text{sat}}$ ( $\mu_B$ )	Energy of excited state (K)	Compound ground state max <sup>m</sup> $\mu_{\text{sat}}$ ( $\mu_B$ )	Free ion		Observed $\mu_{\text{sat}}$ at 38 KOe		Observed		
									$\mu_{\text{eff}}$	$\mu_{\text{sat}}$	4.2 K	1.2 K	$\mu_{\text{eff}}$ 4.2 K	$\mu_{\text{eff}}$ 1.2 K	$\Theta$ (K)
$\text{PrPd}_3$	$\Gamma_5$	2.83	2.0	$\Gamma_3$	0	0	5	2.0	3.58	3.2	0.77	0.98	2.92	2.83	-5
$\text{TbPd}_3$	$\Gamma_3$	0	0	$\Gamma_5^{(1)}$	1.28	0.906	8	< 100 > 7.62 < 111 > 5.85	9.72	9.0	6.31	6.60	13.0	5.7	0
$\text{ErPd}_3$	$\Gamma_6$	5.19	3.0	$\Gamma_8^{(3)}$	6.97	< 100 > 5.67 < 111 > 4.84	2	< 100 > 8.97 < 111 > 7.42	9.58	9.0	7.20	7.52	9.60	7.45	0

value of  $\Theta$  for Pr-Pd alloys depends critically on the Praseodymium content in the region of 25 % Pr.

### 5.2. *TbPd<sub>3</sub>*

The magnetization of a 16.3 mg sphere of *TbPd<sub>3</sub>* has been measured from 1.2 to 10 K in applied magnetic fields varying from 2 to 42 kOe. The inverse of the observed magnetic susceptibility obtained in an applied field of 2.3 kOe as a function of temperature is shown in figure 8. An antiferromagnetic transition clearly occurs at  $\sim 3.5$  K in good agreement with the ordering observed at 3.75 K in the heat capacity results. This transition is more clearly marked than the shallow minimum observed previously [2] in this temperature region but on a different sample. Since the Tb content of both samples is close to 25 % the magnetic behaviour below 4 K must be sensitive to the details of the preparation. The ground level of *TbPd<sub>3</sub>* is  ${}^7F_6$ . Specific heat measurements have shown (section 4.3) that in addition to the exchange interaction which produces antiferromagnetism there is a crystal field present which splits the level into the states given in table 3b. Using the crystal field parameters of table 3c and eq. (18) the magnetic susceptibility as a function of temperature has been calculated. The calculated values of  $1/\chi_m$  are greater than  $1/\chi_{obs}$  between 1 and 10 K but a good fit can be achieved by using eq. (26). In figure 8 the theoretical curve for crystal field parameters of table 3c line (ii) was displaced using  $g = 1.5$  and  $\lambda = 0.49$  g mole/emu; the equivalent high temperature  $\Theta$  being 3.9 K. An equally good fit can be obtained from the crystal field parameters of table 3c line (i) with  $\lambda = 0.50$  g mol/emu. Thus the large exchange displacement makes the observed values insensitive to the choice of crystal field parameters presented by the heat capacity analysis.

The magnetic moment/Tb atom, obtained after correcting the results for the diamagnetism of the matrix, at 4.2 and 1.2 K is shown in figure 9 as a function of the applied magnetic field. Although the curves show that saturation occurs the magnetization is still rising slowly above 40 kOe. The magnetization at 1.2 K exceeds that of 4.2 K above a field of 5 kOe. The value of  $6.2 \mu_B$  at 40 kOe and 1.2 K lies well below the free ion value of  $9 \mu_B$  and clearly reveals the effect of the crystal field.

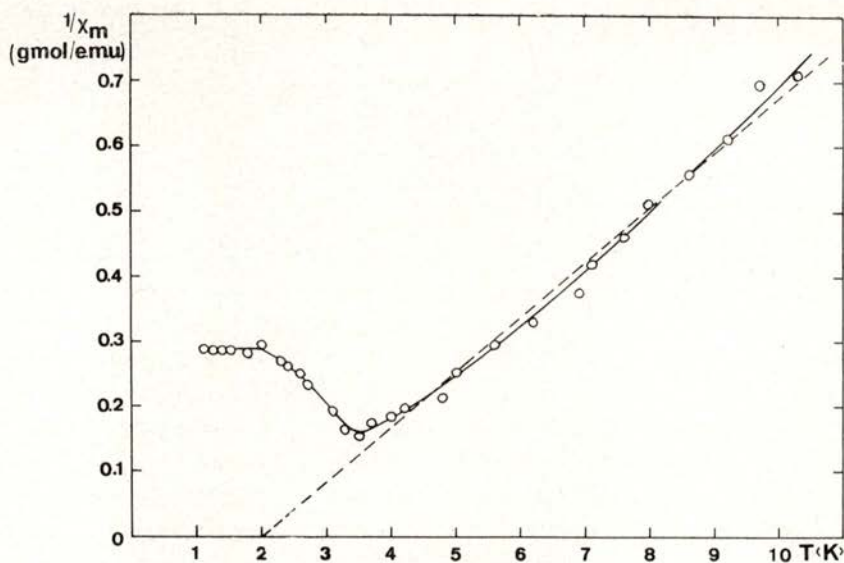


Fig. 8 — The reciprocal of the molar susceptibility ( $\chi_m^{-1}$ ) of  $\text{TbPd}_3$  as a function of temperature from measurements in an applied field of 2.3 kOe; — — — free ion Curie-Weiss relation,  $\Theta = 2$  K.

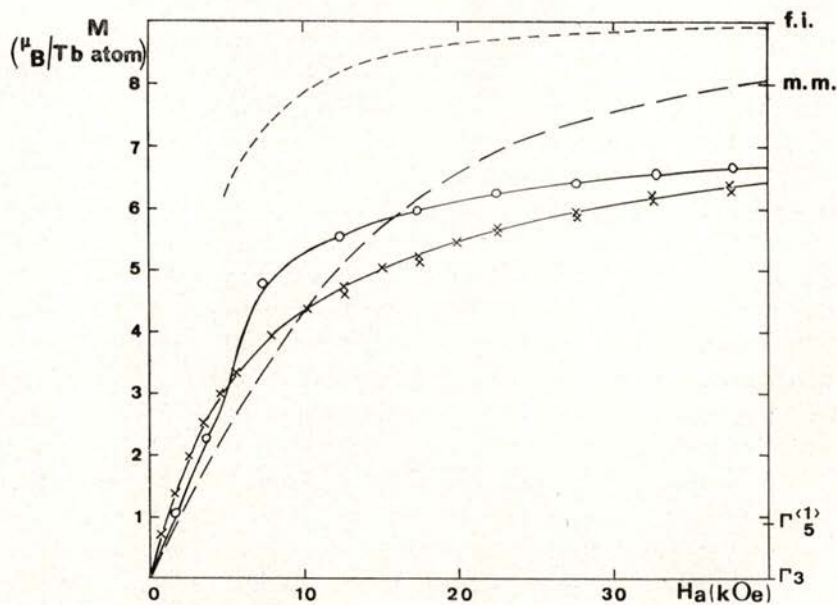


Fig. 9 — The magnetic moment/Tb atom ( $\mu_B$ ) as a function of effective field,  $H_a$ :  $\times$  (4.2 K);  $\circ$  (1.2 K). The curves represent the Brillouin function for  $J = 6$ ;  $g = 3/2$  at 4.2 K (— — —) and 1.2 K (- - -); f.i. = free ion, m.m. = mixed maximum (Bleaney [13]).

### 5.3. $\text{ErPd}_3$

The magnetization of a 16.9 mg sphere of  $\text{ErPd}_3$  has been measured at 4.2 and 1.2 K in effective fields up to 38 kOe and the results are shown in figure 10.

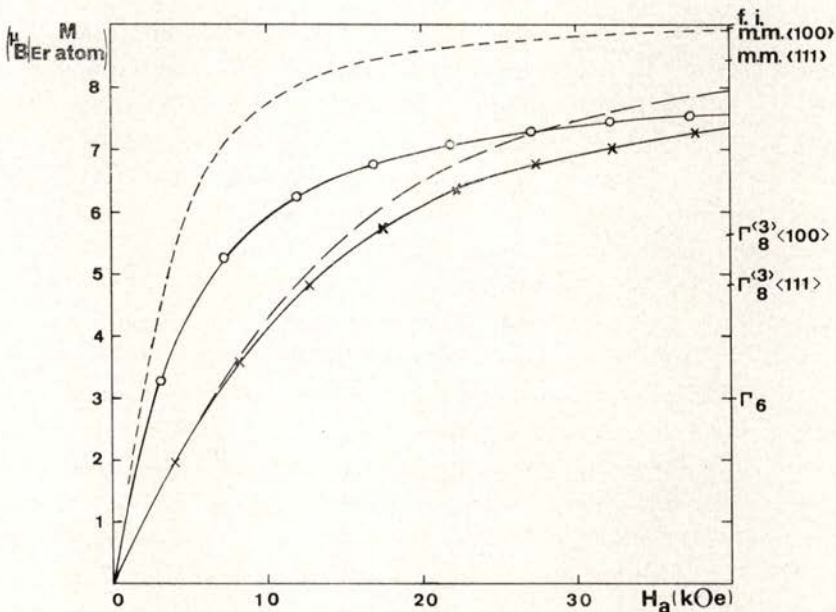


Fig. 10—The magnetic moment/Er atom as a function of effective field  $H_a$ :  $\times$  (4.2 K);  $o$  (1.2 K). The curves represent the Brillouin function for  $J = 15/2$ ,  $g = 6/5$ , at 4.2 K (—) and 1.2 K (---); f.i. = free ion, m.m. = mixed maximum (Bleaney [13]).

The magnetic susceptibility of  $\text{ErPd}_3$  closely follows Curie's law from 4 to 300 K [2] with  $\mu_{\text{eff}}$  close to the free ion value; the initial slope at 4.2 K for this sample agrees with this behaviour but departure occurs at 1.2 K. For  $H_a = 38$  kOe the magnetizations at 4.2 and 1.2 K fall well below the Brillouin values for the free ion. This behaviour suggests that exchange interaction effects are unimportant and the departures are associated with the crystal field. In section 4.4 the specific heat

results also showed that exchange interactions are weak and that any magnetic ordering occurs below 0.22 K. They also showed that the ground state is  $\Gamma_6$  and that the first excited state  $\Gamma_8^{(3)}$  is at 2.0 K. However no information was obtained about the energies of higher levels so that from the knowledge of the separation of  $\Gamma_6$  and  $\Gamma_8^{(3)}$  it was only possible to calculate pairs of corresponding values of  $x$  and  $W$  (or  $A_4 \langle r^4 \rangle$  and  $A_6 \langle r^6 \rangle$ ) (table 4b).

Since the overall separation increases as  $x$  decreases the magnetization in a given direction will take its maximum value for  $x = 1.0$ . In figure 10 only the calculated curves for  $x = 1.0$  and  $x = 0.90$  are shown, since the other values produce intermediate curves. It is obvious that even the smallest energy separation of the higher levels corresponding to  $x = 1.0$  does not produce a large enough magnetization at either 4.2 or 1.2 K for  $H_a = 38$  kOe. We cannot improve this fit by decreasing their separation further without lowering the energy separation of  $\Gamma_6$  and  $\Gamma_8^{(3)}$  and hence spoiling the fit to the specific heat results. Thus it is apparent that the discrepancy is a real effect. In figs 11 and 12 the separate curves of  $x = 1.0$  and 0.90 for the three major crystalline directions are shown and it can be seen that there is considerable anisotropy, with the value in the  $\langle 100 \rangle$  direction exceeding that in the  $\langle 111 \rangle$  direction by 50 % at 40 kOe. In addition the magnetization saturates most easily in the  $\langle 100 \rangle$  direction but the change between 20 kOe and 40 kOe at 1.2 K for the harder directions is only  $\sim 0.4 \mu_B$ , compared with an observed change  $\sim 0.8 \mu_B$ .

Thus the discrepancy between the theoretical curves and the experiment at 38 kOe could be associated with the method used to calculate  $M_p$ . However, it cannot simply be attributed to the approximation adopted for  $M_p$ , since the theoretical curve at 4.2 K lies below the observed values at all fields whereas at 1.2 K it exceeds the observed values for fields less than 15 kOe and at both temperatures in fields over 20 kOe the observed values of  $M/H$  are greater than the calculated ones. This suggests that there may be effects due to crystalline field anisotropy and that the moments may not rotate freely at low temperatures, but may well prefer the  $\langle 100 \rangle$  direction.

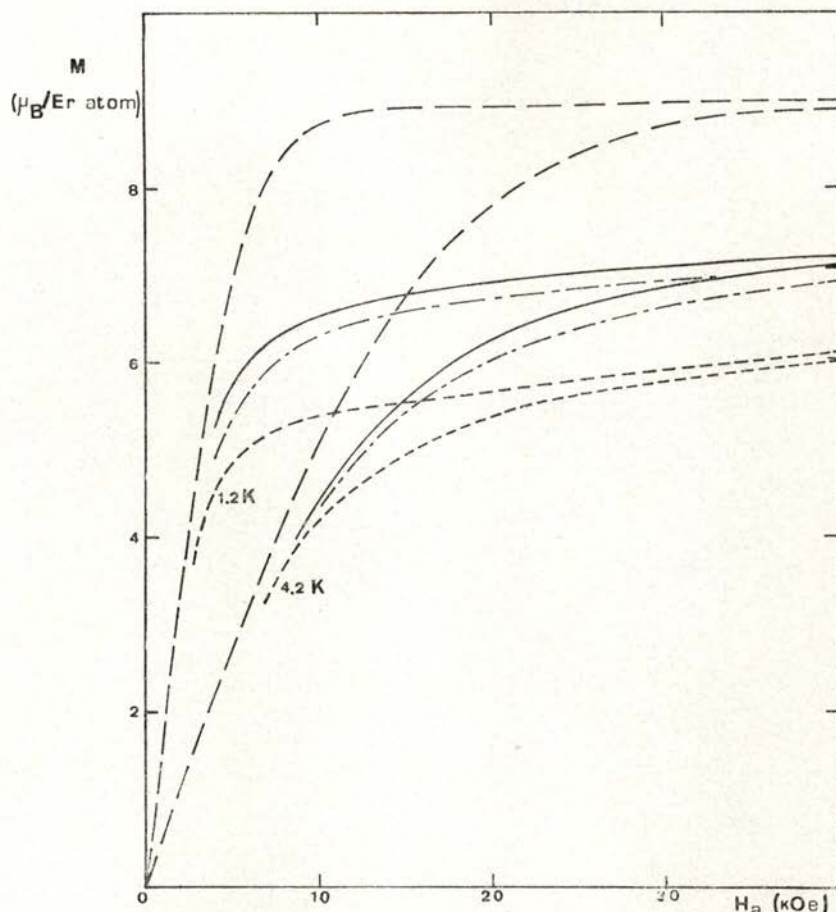


Fig. 11 — Calculated values of  $M_{100}$  (---);  $M_{110}$  (- · -);  $M_{111}$  (·····) and  $M_p$  (—) at 4.2 K and 1.2 K for  $\text{ErPd}_3$ ;  $x = 1.0$ ,  $W = -0.072$ .

Thus the magnetization results on a polycrystalline sample are unable to determine the appropriate pair of crystalline field parameters from table 4b. Clearly measurements on a single crystal of  $\text{ErPd}_3$  are required.

## 6 — DISCUSSION

The magnetic susceptibility measurements of Gardner *et al* [2] showed that the exchange interaction was unimportant in several

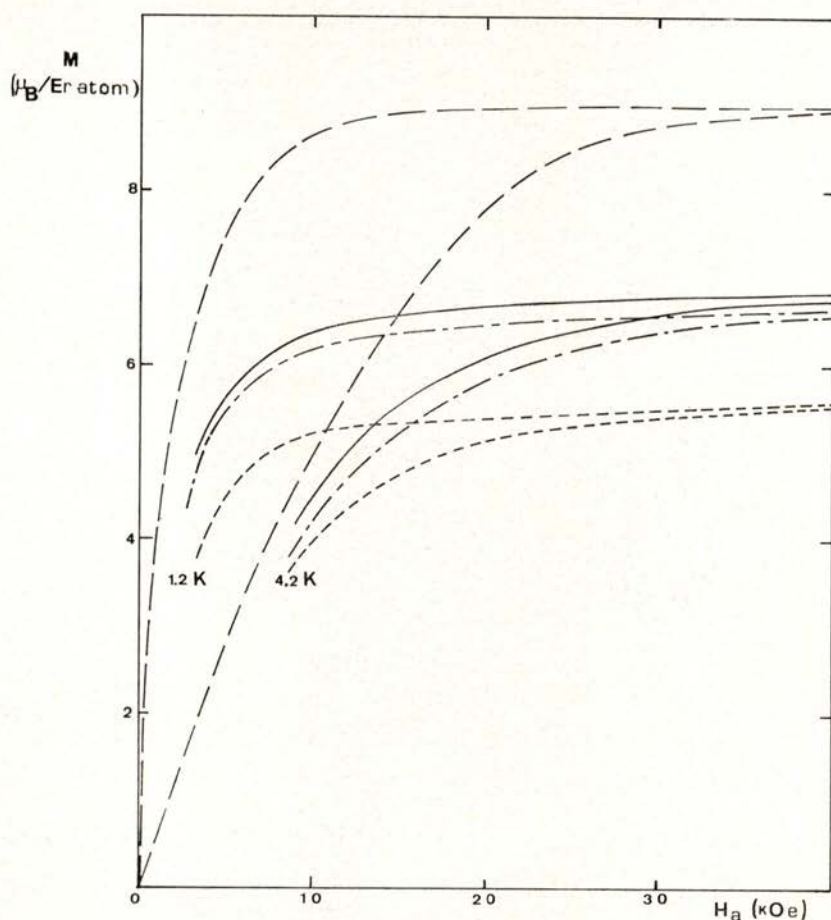


Fig. 12 — Calculated values of  $M_{100}$  (— — —);  $M_{110}$  (— · —);  $M_{111}$  (· · · · ·) and  $M_p$  (—) at 4.2 K and 1.2 K for  $ErPd_3$ :  $x = 0.9$ ,  $W = -0.19$ .

$RPd_3$  phases above 1 K and that the point charge model correctly predicted the ground state if the fourth order term was assumed predominant. Electrical resistivity measurements [23] confirmed the absence of magnetic order above 1 K in many of the phases but the suggestion that  $PrPd_3$  and  $SmPd_3$  magnetically ordered between 3 and 5 K is incorrect and associated with impurities, as suspected by these authors.

Elliot and Hill [23] also considered the possible existence of a Kondo effect in  $LaPd_3$  since they observed a weak minimum in the resistivity at about 4 K. They were inclined to associate

this with the effects of impurities but were unable to rule out the possibility that it might be induced by the Pd atoms.

The magnetic susceptibility measurements [2] which show that LaPd<sub>3</sub> is a diamagnet clearly rule out this latter possibility and the weak minimum must therefore be associated with impurities (as is the observed rise in magnetic susceptibility at low temperatures). Thus instead of introducing the concept of spin fluctuations to account for the anomalous heat capacity behaviour of LaPd<sub>3</sub> observed by Hutchens *et al* [18] we would simply associate it with the presence of impurities. It is not difficult to obtain the small effects observed ( $C_V/R \sim 10^{-2}$  at 5 K) from the presence of rare earth impurities since the specific heat of the magnetic RPd<sub>3</sub> phases is very much greater ( $C_V/R \sim 0.5$  at 5 K).

Now simple point charge calculations have been successful, rather surprisingly, in predicting the crystal field parameters determined from neutron scattering measurements [21] in rare earth compounds. This success has been repeated by Nowik *et al* [24] in YbPd<sub>3</sub> using Mossbauer effect studies. Nowik *et al* [24] reproduced experimental observations of the dependence of the magnetic hyperfine field (and quadrupole interaction) of the <sup>170</sup>Yb nucleus with applied field. These authors used a crystal field calculation to determine the magnetic hyperfine field along three  $\langle 100 \rangle$ ,  $\langle 110 \rangle$  and  $\langle 111 \rangle$  crystalline symmetry axes as a function of applied field and, since the anisotropy was only  $\sim 10\%$ , averaged over these directions, instead of all orientations of applied field, to determine the crystal field parameters for their powder sample. A best fit was achieved using  $B_4/\beta = -12 \pm 1 \text{ cm}^{-1}$  and  $B_6/\gamma = 0.6 \pm 0.6 \text{ cm}^{-1}$ .

Perhaps we should point out that this analysis is identical with the analysis for the magnetisation as a function of applied field and that the experimental observations are equivalent to the measurement of magnetization from 0 to 45 kOe at 4.2 and 1.4 K.

A simple point-charge model calculation (the details are described in section 3) using equations (3) and (4) with  $Z_1 = 0$  (a neutral Pd atom) and with  $Z_2 = 3$  (an unscreened Yb<sup>3+</sup> ion), produces [24] the values  $B_4/\beta = -10.7 \text{ cm}^{-1}$  and  $B_6/\gamma = 0.065 \text{ cm}^{-1}$ . The energy levels from the two determinations are given in

table 7. The agreement between the two sets of values is good, although in the light of our additional comparisons, it may well be fortuitous.

TABLE 7—The energies of the crystal field states of Yb<sup>3+</sup>

State	Degeneracy	Mossbauer Calculated Energy (K)	Point-charge Calculated Energy (K)
$\Gamma_7$	2	0	0
$\Gamma_8$	4	42	32
$\Gamma_6$	2	56	52
Ground level $^2F_{7/2}$			
		x	W(K)
	Mossbauer	0.92	1.96
	point-charge	0.99	- 1.61

This excellent agreement has not been observed using a similar analysis to fit the specific heat and magnetization results obtained on PrPd<sub>3</sub>, TbPd<sub>3</sub> and ErPd<sub>3</sub>. Nor has it proved possible by varying the assumptions about the charges on the neighbouring atoms to obtain satisfactory agreement. Junod *et al* [25] also failed to obtain good agreement with a simple point charge model calculation and the crystal field parameters determined for RN compounds. However, the specific heat results confirmed that the point charge model correctly predicts the ground state, if the fourth order term is predominant. They also showed that probably the exchange field mixes the two lowest states in TbPd<sub>3</sub> so as to produce in second order a magnetic  $\Gamma_3$  ground state in the  $\langle 100 \rangle$  direction.

Mossbauer measurements on TbPd<sub>3</sub> (Longworth, private communication) also show that ordering takes place below 4 K. Details of the ordering have been investigated using neutron scattering (Wedgwood, private communication) and it has been established that it is much more complex than that observed in TbPt<sub>3</sub> [26]. In addition, using neutron techniques similar to

those of Turberfield *et al* [21], Wedgwood (private communication) has been able to make a detailed study of the states produced by the crystalline field and thus complement the results obtained from these measurements.

#### ACKNOWLEDGEMENTS

We would like to thank T F Smith, in particular, for his vital support, B Bleaney, R W Hill, G Longworth, R Levi and F A Wedgwood for valuable discussions, and D Kells and N Nambudripad for assistance with the measurements and analysis of the results. We would also like to thank B D Dunlop for sending us a preprint of ref [24]. One of us (JMMS) would like to thank the Science Research Council (UK) for a post doctoral grant.

#### REFERENCES

- [1] McMASTERS, O. D. and GSCHNEIDER, JR, K. A., *Nuclear Metallurgy*, **10**, 93 (1964).
- [2] GARDNER, W. E., PENFOLD, J., SMITH, T. F., HARRIS, I. R., *J. Phys.*, **F2**, 133 (1972).
- [3] BUSCHOW, K. H. J., DE WIJN, H. W., and VAN DIEPEN, A. H., *J. Chem. Phys.*, **50**, 137 (1969).
- [4] HUTCHENS, R. D., and WALLACE, W. E., *J. Solid State Chem.*, **3**, 564 (1971).
- [5] GARDNER, W. E., and SMITH, T. F., *Progr. Vacuum Microbalance Tech.*, **1**, 155, edited by T. Gast and E. Robins, Heyden and Son Limited (1972).
- [6] MACHADO DA SILVA, J. M., D. Phil Thesis, Oxford (1970).
- [7] KEESOM, P. H. and PEARLMAN, N., *Encyclopaedia of Physics*, **14**, 282 (1956).
- [8] STEVENS, K. W. H., *Proc. Phys. Soc. (London)*, **A65**, 209 (1952).
- [9] HUTCHINGS, M. T., *Solid State Physics*, **16**, 277 (1964).
- [10] LEA, K. R., LEASK, M. J. M., and WOLF, W. P., *J. Phys. Chem. Solids*, **23**, 1381 (1962).
- [11] HILL, R. W., D. Phil Thesis, Oxford University, p. 26 (1952).
- [12] CHAN, S. K., *J. Phys. Chem. Solids*, **32**, 1111 (1971).
- [13] BLEANEY, B., *Proc. Roy Soc. (London)*, **A276**, 19 (1963).
- [14] SCHUMACHER, D. P., and HOLLINGSWORTH, C. A., *J. Phys. Chem. Solids*, **27**, 749 (1966).
- [15] TRAMMELL, G. T., *Phys. Rev.*, **131**, 932 (1963).
- [16] MACHADO DA SILVA, J. M., *Solid State Comm.*, **28**, 857 (1978).
- [17] MACHADO DA SILVA, J. M., *Journal de Physique*, **152**, 40 (1979).

- [18] HUTCHENS, R. D., RAO, V. U. S., GREEDAN, J. E., and CRAIG, R. S, *Proc., 9th Rare Earth Research Conference*, Blacksburg, Virginia (Editor P. E. Field), 680 (1971).
- [19] DONIACH, S., and ENGELSBERG, S., *Phys., Rev. Lett*, **17**, 750 (1960).
- [20] ROBINSON, W. K., and FRIEDBERG, S. A., *Phy. Rev.*, **117**, 402 (1960).
- [21] TURBERFIELD, K. C., PASSEL, L., BIRGENAU, R. J. and BUCHER, E., *J. App. Phys.*, **42**, 1746 (1971).
- [22] FURRER, A. and PURWINS, H. G., *J. Phys.*, **C9**, 1491 (1976).
- [23] ELLIOTT, R. O. and HILL, H. H., *Proc. 9th Rare Earth Research Conference*, Blacksburg, Virginia (Editor P. E. Field), (1971).
- [24] NOWIK, I., DUNLOP, B. D. and KALVIUS, G. M., *Phys. Rev.*, **B6**, 1048 (1972).
- [25] JUNOD, P., MENTH, A. and VOGT, O., *Phys. Kondens Materie*, **8**, 323 (1969).
- [26] NERESON, N. and ARNOLD, G., *J. Chem. Phys.*, **53**, 2818 (1970).